

M. Cakmak, I.I. Ozturk*, C.N. Banti*, M. Manoli, E. Moushi^a, A.J. Tasiopoulos, A.M. Grzeńkiewicz, M. Kubicki and S.K. Hadjikakou*

Bismuth(III) bromide-thioamide complexes: synthesis, characterization and cytotoxic properties

<https://doi.org/10.1515/mgmc-2018-0035>

Received June 23, 2018; accepted August 13, 2018; previously published online September 21, 2018

Abstract: New bismuth(III) bromine compounds of the heterocyclic thioamides were prepared and structurally characterized. The reaction of heterocyclic thioamides with bismuth(III) bromide resulted in the formation of the $\{[\text{BiBr}_2(\mu_2\text{-Br})(\text{MMI})_2]_2 \cdot \text{CH}_3\text{COCH}_3 \cdot \text{H}_2\text{O}\}$ (**1**), $\{[\text{BiBr}_2(\text{MBZIM})_4] \cdot \text{Br} \cdot 2\text{H}_2\text{O}\}$ (**2**), $\{[\text{BiBr}_2(\mu_2\text{-Br})(\text{tHPMT})_2]_2 \cdot \text{CH}_3\text{CN}\}$ (**3**), $\{[\text{BiBr}_2(\mu_2\text{-Br})(\text{PYT})_2]_2 \cdot \text{CH}_3\text{CN}\}$ (**4**) and $\{[\text{BiBr}_2(\mu_2\text{-Br})(\text{MBZT})_2]_2 \cdot 2\text{CH}_3\text{OH}\}$ (**5**) complexes (MMI: 2-mercapto-1-methylimidazole, MBZIM: 2-mercaptobenzimidazole, tHPMT: 2-mercapto-3,4,5,6-tetrahydro-pyrimidine, PYT: 2-mercaptopyridine and MBZT: 2-mercaptobenzothiazole). The complexes **1–5** were characterized by melting point (m.p.), elemental analysis (e.a.), molar conductivity, Fourier-transform infrared (FT-IR), Fourier-transform Raman (FT-Raman), nuclear magnetic resonance (¹H and ¹³CNMR) spectroscopy, UV-Vis spectroscopy and thermogravimetric-differential thermal analysis (TG-DTA). The molecular structures of **1–5** were determined by single-crystal X-ray diffraction. Complex **2** is a first ionic mononuclear octahedral bismuth(III) bromide, while the complexes **1, 3–5** are the first examples of dinuclear bismuth(III) bromide derivatives. Complexes **1–5** were evaluated in terms of their *in vitro* cytotoxic activity

against human adenocarcinoma breast (MCF-7) and cervix (HeLa) cells. The toxicity on normal human fetal lung fibroblast cells (MRC-5) was also evaluated. Moreover, the complexes **1–5** and free heterocyclic thioamide ligands were studied upon the catalytic peroxidation of the linoleic acid by the enzyme lipoxygenase (LOX).

Keywords: biological inorganic chemistry; bismuth(III) bromide; cytotoxicity; thioamides.

Introduction

Presently, the medicinal application of bismuth(III) compounds is focused on the antibacterial and anticancer metallodrugs (Yang and Sun, 2007). Thus, bismuth(III) halide dithiocarbamate complexes of the general formula $\text{BiX}_n(\text{S}_2\text{CNR}_2)_{3-n}$, ($n=0, 1$ and 2 , $\text{X}=\text{Cl}, \text{Br}$ or I) have proven to display extremely strong cytotoxic activity against human breast adenocarcinoma (MCF-7) cells, while their IC_{50} values lie in the range of nanomolar (Ozturk et al., 2014a,b; Arda et al., 2016). Bismuth(III) thiosemicarbazone complexes also showed effective cytotoxic activity against cancerous cell lines (Li et al., 2012a,b; Zhang et al., 2014).

The enzyme lipoxygenase (LOX) participates in the mechanism of inflammation, catalyzing the oxidation of arachidonic acid to leukotrienes in an essential mechanism for cell life (Xanthopoulou et al., 2008; Ozturk et al., 2010; Poyraz et al., 2011). LOX has been investigated as a potent target for the development of new metallodrugs against cancerous cells as it has been associated with the antiproliferative activity by the induction of apoptosis in tumor cells (Poyraz et al., 2011).

In the course of our studies towards the development of effective chemotherapeutic agents (Hadjikakou et al., 2005; Ozturk et al., 2007, 2009, 2010, 2011, 2012a,b, 2013, 2014a,b, 2017; Xanthopoulou et al., 2008; Balas et al., 2011; Poyraz et al., 2011; Shpakovsky et al., 2012; Banti et al., 2016; Urgut et al., 2016a,b; Yazar et al., 2018) we describe here the synthesis and characterization of the complexes $\{[\text{BiBr}_2(\mu_2\text{-Br})(\text{MMI})_2]_2 \cdot \text{CH}_3\text{COCH}_3 \cdot \text{H}_2\text{O}\}$ (**1**), $\{[\text{BiBr}_2(\text{MBZIM})_4] \cdot \text{Br} \cdot 2\text{H}_2\text{O}\}$ (**2**), $\{[\text{BiBr}_2(\mu_2\text{-Br})$

^aPresent address: Department of Life Sciences, The School of Sciences, European University Cyprus, 1516 Nicosia, Cyprus.

*Corresponding authors: I.I. Ozturk, Department of Chemistry, Namik Kemal University, Tekirdag 59030, Turkey, e-mail: iiozturk@nku.edu.tr; and C.N. Banti and S.K. Hadjikakou, Section of Inorganic and Analytical Chemistry, Department of Chemistry, University of Ioannina, Ioannina 45110, Greece, e-mail: cbanti@cc.uoi.gr (C.N. Banti); shadjika@uoi.gr (S.K. Hadjikakou)

M. Cakmak: Department of Chemistry, Namik Kemal University, Tekirdag 59030, Turkey

M. Manoli, E. Moushi and A.J. Tasiopoulos: Department of Chemistry, University of Cyprus, Nicosia 1678, Cyprus

A.M. Grzeńkiewicz and M. Kubicki: Department of Chemistry, A. Mickiewicz University, ul. Umultowska 89b, Poznan 61-614, Poland

(tHPMT)₂ · CH₃CN} (3), {[BiBr₂(μ₂-Br)(PYT)₂]₂ · CH₃CN} (4) and {[BiBr₂(μ₂-Br)(MBZT)₂]₂ · 2CH₃OH} (5) using the heterocyclic thioamide ligands (Scheme 1). In order to rationalize the hindrance due to steric effects and the electronic factors that govern the biological activity, many compounds of the main group of metal ions (Sn(IV), Sb(III/IV), Bi(III) etc.) (Hadjikakou et al., 2005; Ozturk et al., 2007, 2009, 2010, 2011, 2012a,b, 2013, 2014a,b, 2017; Xanthopoulou et al., 2008; Balas et al., 2011; Poyraz et al., 2011; Shpakovsky et al., 2012; Banti et al., 2016; Urgut et al., 2016a,b; Yarar et al., 2018) with various types of ligands, such as Thioamides, Dithiocarbamates, the Non-Steroidal Anti-inflammatory Drugs (NSAID), aspirin, salicylic acid, naproxen, etc. were synthesized and characterized.

The present manuscript describes the recent results obtained in bismuth(III) bromide. These results are compared with those previously reported from our group in relation with the drug cisplatin, which is in clinical use (Table 2). Conclusions will be attempted upon changing either the halogen counter anion (Cl, Br and I) or the ligand type (thioamides, dithiocarbamates). Among thioamides, the electronic effect is arising from thiourea derivatives with 5-member ring imidazole, benzimidazole and benzothiazole and 6-member ring tetrahydro pyrimidine and pyridine (Scheme 1). The *in vitro* cytotoxicity of the compounds was tested against the cancerous and non-cancerous cell lines. The antioxidant behaviors of these compounds are also evaluated with their influence upon

the catalytic peroxidation of linoleic acid by the enzyme of lipoxygenase (LOX).

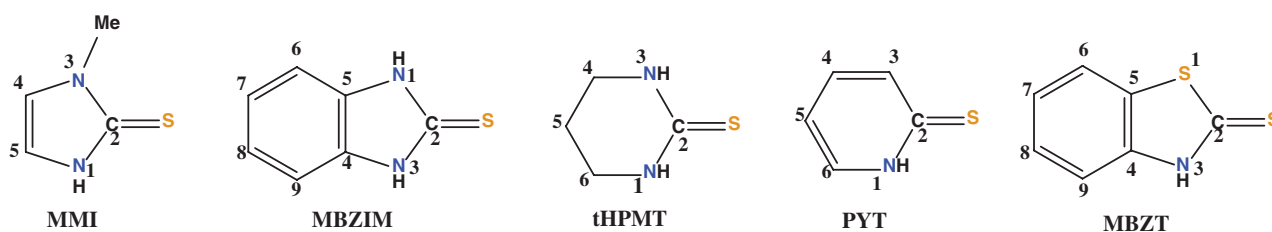
Results and discussion

General aspects

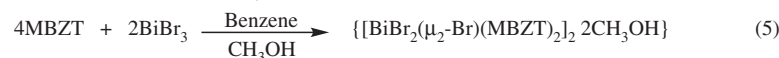
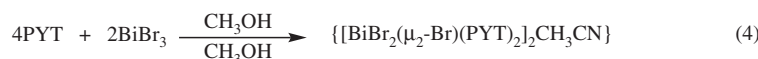
The reactions of bismuth(III) bromide with the heterocyclic thioamides (MMI: 2-mercapto-1-methylimidazole, MBZIM: 2-mercaptobenzimidazole, tHPMT: 2-mercapto-3,4,5,6-tetrahydro-pyrimidine, PYT: 2-mercaptopyridine, MBZT: 2-mercaptobenzothiazole) in 1:2 (M:L) molar ratio, result in the isolation of the complexes {[BiBr₂(μ₂-Br)(MMI)₂]₂ · CH₃COCH₃ · H₂O} (1), {[BiBr₂(MBZIM)₄]₂ · Br · 2H₂O} (2), {[BiBr₂(μ₂-Br)(tHPMT)₂]₂ · CH₃CN} (3), {[BiBr₂(μ₂-Br)(PYT)₂]₂ · CH₃CN} (4) and {[BiBr₂(μ₂-Br)(MBZT)₂]₂ · 2CH₃OH} (5) (Scheme 2). Crystals of 1–5, which are suitable for X-ray diffraction (XRD), were grown through the slow evaporation of the solutions. The compounds were characterized by e.a., FT-IR, FT-Raman, ¹H, ¹³C NMR, UV, TG-DTA and single crystal by XRD crystallography.

Vibrational spectroscopy

The characteristic vibration bands of 1–5 and their ligands are summarized in Table S1. Significant changes between



Scheme 1: The molecular formulae of thioamide ligands used in this work.



Scheme 2: The synthesis of bismuth(III) bromide complexes with thioamides (1–5).

the IR spectra of the complexes towards their ligands were observed. The IR spectra of **1–5** show distinct vibrational bands at 1468–1284 (**1**), 1491–1346 (**2**), 1595–1203 (**3**), 1508–1124 (**4**) and 1491–1331 cm^{-1} (**5**), respectively, which are attributed to the $\nu(\text{CN})$ vibrations (Thioamide I and II bands) (Supplementary Figures S1–S5). The vibration bands at 1088–742 (**1**), 1005–752/741 (**2**), 1111–623 (**3**), 1034–721 (**4**) and 1007–600 cm^{-1} (**5**) are assigned to the $\nu(\text{CS})$ vibrations (Thioamide III and IV bands) (Figures S1–S5). The amide N-H bond stretching vibrations were observed in the region of 3265–3068 cm^{-1} in **1–5** (Figures S1–S5). The corresponding thioamide bands of the free ligands are 1456, 1273, 1084 and 737 cm^{-1} for MMI; 1508, 1354, 1014 and 694 cm^{-1} for MBZIM; 1552, 1192, 1065 and 642 cm^{-1} for tHPMT; 1570, 1254, 1132 and 727 cm^{-1} for PYT and 1495, 1319, 1032 and 667 cm^{-1} for MBZT (Ozturk et al., 2007, 2009, 2010) (Figures S6–S10).

Further information about the bonding type of **1–5** was obtained by FT-Raman spectroscopy (Ozturk et al., 2007, 2009, 2010, 2011, 2012a,b, 2013, 2014a,b, 2017; Urgut et al., 2016a,b; Yarar et al., 2018) (Supplementary Table S1, Figures S11–S15). The metal-sulfur vibration bands can be found between 200 and 350 cm^{-1} (Ozturk et al., 2007, 2009, 2010, 2011, 2012a,b, 2013, 2014a,b, 2017; Urgut et al., 2016a,b; Yarar et al., 2018). The new peaks at 234 (**1**), 205 (**2**), 231 (**3**), 253 (**4**) and 228 cm^{-1} (**5**) are assigned at the Bi-S bond. The terminal Bi-Br vibration band appears at 187 (**1**), 148 (**2**), 162 (**3**), 165 (**4**) and 203 cm^{-1} (**5**), respectively. The bands at 168 (**1**), 142 (**3**), 145 (**4**) and 178 cm^{-1} (**5**) are attributed to the Bi-Br terminal bond. The bridging Bi-Br-Bi vibration bands for **1–5** appear at 105 (**1**), 108 (**3**), 117 (**4**) and 139 cm^{-1} (**5**), respectively. On the one hand, compound **2** is monomeric as the terminal Bi-Br and the Bi-S vibrations bands appeared in the Raman spectrum. Complexes **1, 3–5** on the other hand, have bridging Bi-Br-Bi vibration bands and terminal vibrations; therefore, they are classified as dimmers.

Given that the assignment of the vibrational spectra of **1–5** was made using the molecular structures, which were determined from the single crystal XRD data (see Section ‘Crystal and molecular structures’), the retention of the formulae is deduced in the solid state for these samples. This is required for the samples’ purity verification.

TG-DTA analysis

The thermal stability of **1–5** was analyzed by thermal gravimetry-differential thermal analysis (TG-DTA) under nitrogen atmosphere (Figure S16). After the releasing of the solvents from the crystal lattice, complexes **1–5** are stable up to 206°C (**1**), 270°C (**2**), 150°C (**3**), 120°C (**4**) and

150°C (**5**), respectively. The corresponding TG-DTA diagrams for compounds **1–5** (206°C–940°C) (**1**), 100°C–825°C (**2**), 106°C–983°C (**3**), 110°C–983°C (**4**) and 128°C–983°C (**5**) involve 100% (**1**), 98.91% (**2**), 97.95% (**3**), 100% (**4**) and 97.20% (**5**) mass losses, respectively.

UV-Vis spectroscopy

The UV-Vis absorption spectra of the heterocyclic thioamide ligands as well as the corresponding ones of their bismuth(III) bromide complexes **1–5** were recorded in the DMSO solution (Figure S17). The absorption bands for complexes **1, 3** and **4** were observed around 300–450 nm, which can be attributed to the intra-ligand electrons’ transitions.

NMR spectroscopy

The ^1H and ^{13}C -NMR spectra of **1–5** and their ligands (Figures S18–S37) were recorded in DMSO- d_6 . Their chemical shifts are summarized in Table S2. The resonance signals at 12.26 (**1**), 12.57 (**2**), 8.07 (**3**), 13.66 (**4**) and 13.80 ppm (**5**), respectively (Figures S18–S27), are attributed to the amine protons of **1–5**. The ^1H NMR chemical shift values of **1–5** are almost similar to those of the corresponding ligands. The $^{13}\text{C}(=\text{S})$ resonance signals in the ^{13}C NMR spectra of **1–5** are observed at 159.57 (**1**), 168.92 (**2**), 174.11 (**3**), 176.43 (**4**) and 190.72 ppm (**5**), respectively (Figures S28–S37). The ^{13}C NMR spectra of **1–5** showed the 1–3 ppm up-field shift for the C=S carbon due to complexation. Small shifts in the NMR spectra were also observed for antimony(III) complexes with thioamides or thiones (Ozturk et al., 2011, 2012a,b, 2013, 2014a,b, 2017; Urgut et al., 2016a,b; Yarar et al., 2018).

The assignment of the NMR spectra in the solution was again made using the molecular structures (see Section ‘Crystal and molecular structures’), and therefore, the retention of the formulae is deduced in the solutions. This is required for the further biological studies.

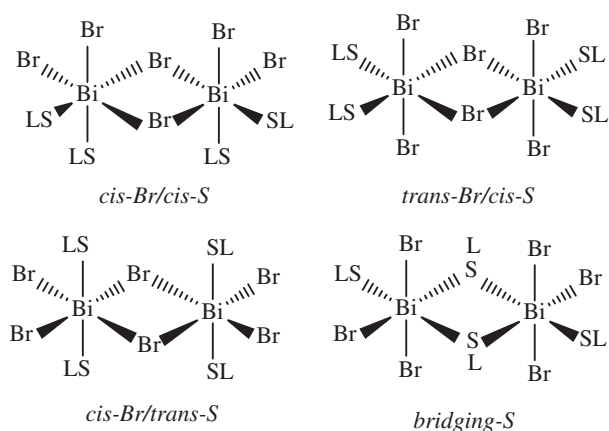
Crystal and molecular structures of $\{[\text{BiBr}_2(\mu_2\text{-Br})(\text{MMI})_2]_2 \cdot \text{CH}_3\text{COCH}_3 \cdot \text{H}_2\text{O}\}$ (**1**), $\{[\text{BiBr}_2(\text{MBZIM})_4] \cdot \text{Br} \cdot 2\text{H}_2\text{O}\}$ (**2**), $\{[\text{BiBr}_2(\mu_2\text{-Br})(\text{tHPMT})_2]_2 \cdot \text{CH}_3\text{CN}\}$ (**3**), $\{[\text{BiBr}_2(\mu_2\text{-Br})(\text{PYT})_2]_2 \cdot \text{CH}_3\text{CN}\}$ (**4**) and $\{[\text{BiBr}_2(\mu_2\text{-Br})(\text{MBZT})_2]_2 \cdot 2\text{CH}_3\text{OH}\}$ (**5**)

Structural reports on bismuth(III) bromide complexes with ligands containing sulfur donor atoms (either thiones

or thioureas) are already known (Li and Li, 2014; Srinivas et al., 2015, 2016). Bismuth(III) bromide complexes with thione adopt octahedral (O_h), square pyramidal (SP) and pseudo-trigonal bipyramidal (ψ -TBP) geometries. The pseudo-trigonal bipyramidal bismuth(III) bromide complexes have a mononuclear core (e.g. [(IPr=S)BiBr₃]·CHCl₃ (Srinivas et al., 2015)), while the octahedral and square pyramidal bismuth(III) bromide complexes have a binuclear core (e.g. [(mbit)Bi(Br)₂(μ₂-Br)₂] (mbit: 3,3'-methylenebis(1-methyl-1*H*-imidazol-3-ium), [(mbpit)Bi(Br)₂(μ₂-Br)₂]·CH₃CN (mbpit: 3,3'-methylenebis(1-isopropyl-1*H*-imidazol-3-ium), [(IMesS)Bi(Br)₂(μ₂-Br)₂]·4CHCl₃ (Srinivas et al., 2016).

Binuclear bismuth(III) complexes with octahedral geometry exhibit four different stereoisomers (Scheme 3), (a) those with two sulfur atoms and two halogen atoms in the cis-orientation and two bismuth atoms bridged to each other by two halogen atoms; (b) those with two sulfur atoms in the cis-position and two halogen atoms in trans-position to each other, while the two bismuth atoms are bridged by two halogen atoms; (c) those with two sulfur atoms in the trans-position and two halogen atoms in the cis-position, while the two bismuth atoms are connected to each other by the two halogen bridges, (d) those with three halogen atoms in the meridional-position and two bismuth atoms, which are connected to each other by two sulfur bridges. However, the binuclear bismuth(III) bromide complexes with octahedral geometry reported up to now have cis-sulfur/trans halogen arrangements (Srinivas et al., 2016).

The structures of **1–5** were determined by single crystal XRD. The selected interatomic distances (Å) and interatomic angles for **1–5** are reported in Table 1. The molecular diagrams of **1–5** are shown in Figures 1–5, respectively.



Scheme 3: The possible stereoisomers adopted by bismuth(III) complexes with octahedral geometry.

Complex **1** is crystallized in the orthorhombic space group $Cmc2_1$, **3** and **4** in the monoclinic space group $C2/c$ and **5** in the triclinic space group $\bar{P}1$. Compounds **1**, **3–5** are isostructural, while their structures constitute the first structurally characterized dinuclear bismuth(III) bromide derivatives with a bismuth:ligand ratio of 1:2. The complexes **1**, **3–5** are dimeric with a center of inversion in the middle of the Bi₂(μ-Br)₂ core in the solid state. The bismuth atoms expose a slightly distorted octahedral geometry. Each bismuth atom is coordinated by two sulfur atoms and four bromine atoms. Two of the bromine atoms are bridging while the other two bromine atoms are bound terminally to bismuth atoms.

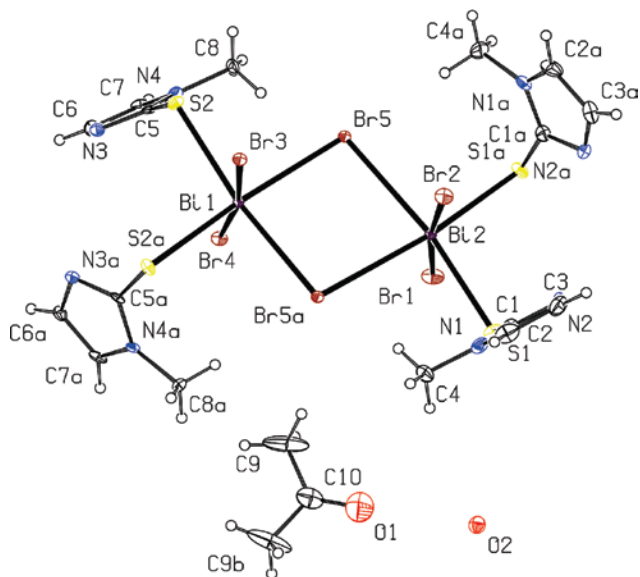
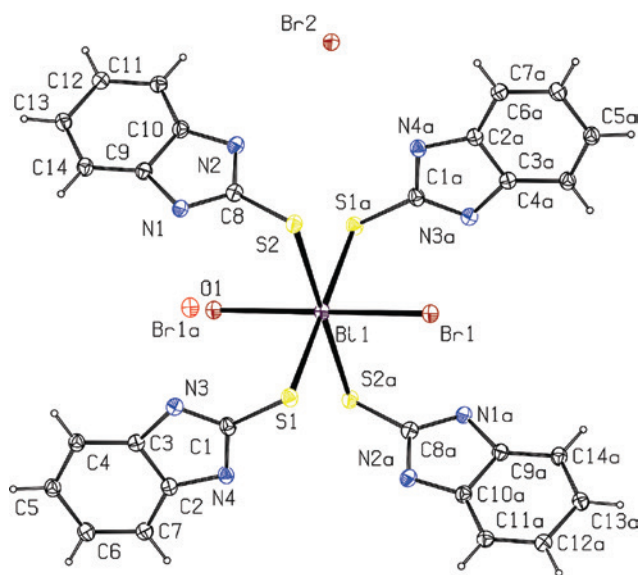
The configuration of **1**, **3** and **4** is *cis-sulfur/trans-bromide* arrangement, while the corresponding one of **5** is *trans-sulfur/cis-bromide* arrangement (Scheme 3). The crystal structure of **1**, **3–5** is further stabilized by hydrogen bonding and weak electrostatic interactions (e.g. S···Br, S···S, C···C, C···H). These interactions make up a 3D supramolecular framework.

Complex **2** is a mononuclear ionic salt in the solid state and it is crystallized in monoclinic space group $P2_1/c$. To the best of our knowledge, **2** is the first ionic mononuclear octahedral bismuth(III) bromide complex structurally characterized. The ionic compound contains the [BiS₄Br₂]⁺ cation, while a bromide serves as counter anion. The coordination number of bismuth in **2** is six, where the equatorial plane is setup by four sulfur atoms from the thione ligands, while the axial positions are occupied by two bromide ions. A third bromide counter ion neutralizes the complex. The basal interatomic angles in the cation are close to the ideal octahedral values. The neighbouring monomeric octahedral molecules are linked by hydrogen bonding and weak electrostatic interactions (e.g. Bi···Br, Br···S, C···C). Consequently, these bonding interactions lead to the 3D supramolecular framework.

The Bi-Br interatomic distances in **1–5** vary from 2.684(1) (Bi1-Br3(**3**)) to 3.117(1) (Bi1-Br1_a(**5**)) Å. These interatomic distances are in agreement with the corresponding interatomic distances observed in the known bismuth(III) bromide complexes (Li and Li, 2014; Ozturk et al., 2014a,b; Srinivas et al., 2015, 2016). Similarly, the Bi-S interatomic distances vary from 2.707(3) (Bi1-S2A (**3**)) to 2.966(2) (Bi1-S1 (**5**)) Å in **1–5**. The Bi-S interatomic distances are comparable with those found in the known bismuth(III) thione complexes (Li and Li, 2014; Ozturk et al., 2014a,b; Srinivas et al., 2015, 2016; Arda et al., 2016; Yazar et al., 2018). The C=S interatomic distances in **1–5** vary from 1.678(1) (**5**) to 1.744(1) (**4**) Å. These bonds are longer than those observed in the free ligands (MMI: 1.681 Å, MBZIM: 1.684 Å, tHPMT: 1.722 Å,

Table 1: The selected interatomic distances (Å) and interatomic angles (°) for the bismuth(III) bromide complexes 1–5.

1	2	3	4	5					
Interatomic distances									
Bi1-S2	2.758(3)	Bi1-S1	2.844(3)	Bi1-S2A	2.707(3)	Bi1-S2A	2.716(2)	Bi1-S1	2.966(2)
Bi2-S1	2.710(3)	Bi1-S2	2.845(3)	Bi1-S2B	2.721(2)	Bi1-S2B	2.745(4)	Bi1-S3	2.709(2)
Bi1-Br3	2.937(1)	Bi1-Br1	2.809(1)	Bi1-Br1	2.958(1)	Bi1-Br1	2.718(1)	Bi1-Br1	2.991(1)
Bi1-Br4	2.725(1)	S1-C1	1.730(1)	Bi1-Br3	2.698(1)	Bi1-Br3	2.964(1)	Bi1-Br2	2.761(1)
Bi1-Br5	2.963(1)	S2-C8	1.722(1)	Bi1-Br2	3.001(1)	Bi1-Br2	2.947(1)	Bi1-Br3	2.684(1)
Bi2-Br1	2.851(1)			Bi1-Br2 _a	3.030(1)	Bi1-Br2 _a	3.026(1)	Bi1-Br1 _a	3.117(1)
Bi2-Br2	2.749(1)			S2A-C2A	1.736(9)	S2A-C2A	1.744(1)	S1-C1	1.678(1)
Bi2-Br5	3.090(1)			S2B-C2B	1.737(1)	S2B-C2B	1.722(1)	S3-C8	1.711(9)
S1-C1	1.730(1)								
S2-C5	1.726(1)								
Interatomic angles									
Br1-Bi2-Br2	172.3(5)	Br1-Bi1-Br1 _a	180.0	Br1-Bi1-Br3	164.2(4)	Br1-Bi1-Br3	168.3(5)	Br3-Bi1-Br1	94.7(3)
S1-Bi2-Br5	171.4(6)	S1-Bi1-S1 _a	180.0	S2A-Bi1-Br2 _a	172.7(6)	S2A-Bi1-Br2 _a	177.5(1)	Br3-Bi1-Br2	90.6(3)
Br1-Bi2-Br5	94.4(4)	S2-Bi1-S2 _a	180.0	S2B-Bi1-Br2	174.8(7)	S2B-Bi1-Br2 _a	85.3(7)	Br2-Bi1-Br1	171.3(3)
Br1-Bi2-S1	81.9(6)	Br1-Bi1-S1	86.6(6)	Br1-Bi1-S2A	76.8(6)	Br1-Bi1-S2A	91.6(7)	Br3-Bi1-Br1 _a	179.3(3)
Br2-Bi2-Br5	91.4(3)	Br1-Bi1-S1 _a	93.3(6)	Br1-Bi1-S2B	74.6(6)	Br1-Bi1-S2B	95.3(7)	Br2-Bi1-Br1 _a	89.0(3)
Br2-Bi2-S1	92.9(6)	Br1-Bi1-S2	86.0(6)	Br1-Bi1-Br2 _a	99.1(4)	Br1-Bi1-Br2	90.9(5)	Br1-Bi1-Br1 _a	85.5(3)
Br3-Bi1-Br4	171.1(5)	Br1-Bi1-S2 _a	93.9(6)	Br1-Bi1-Br2	104.0(3)	Br1-Bi1-Br2 _a	87.5(4)	Bi1-Br1-Bi1 _a	94.4(3)
S2-Bi1-Br5	88.6(6)	S1-Bi1-S2	90.8(7)	Br3-Bi1-S2A	95.5(6)	Br3-Bi1-S2A	78.9(7)	Br3-Bi1-S3	92.6(5)
Br3-Bi1-Br5	90.6(3)	S1-Bi1-S2 _a	89.1(7)	Br3-Bi1-S2B	93.0(5)	Br3-Bi1-S2B	79.2(7)	S3-Bi1-Br2	96.2(5)
Br3-Bi1-S2	82.3(5)			Br3-Bi1-Br2	89.1(3)	Br3-Bi1-Br2	95.6(5)	Br3-Bi1-S1	92.4(5)
Br4-Bi1-Br5	95.8(3)			Br3-Bi1-Br2 _a	89.7(4)	Br3-Bi1-Br2 _a	102.1(4)	S3-Bi1-S1	167.1(6)
Br4-Bi1-S2 _a	91.8(5)			S2A-Bi1-S2B	97.6(9)	S2A-Bi1-S2B	97.0(1)	Br2-Bi1-S1	95.4(5)
				Br2-Bi1-Br2 _a	88.3(4)	Br2-Bi1-Br2 _a	88.6(5)	S3-Bi1-Br1	76.8(5)
				Bi1-Br2-Bi1 _a	91.6(4)	Bi1-Br2-Bi1 _a	91.3(5)	S1-Bi1-Br1	91.0(5)

**Figure 1:** The molecular diagram of $\{[\text{BiBr}_2(\mu_2\text{-Br})(\text{MMI})_2] \cdot \text{CH}_3\text{COCH}_2 \cdot \text{H}_2\text{O}\}$ (1).**Figure 2:** The molecular diagram of $\{[\text{BiBr}_2(\text{MBZIM})_4] \cdot \text{Br} \cdot 2\text{H}_2\text{O}\}$ (2).

PYT: 1.692 Å and MBZT: 1.668 Å) (Ohms et al., 1982; Ravikuma et al., 1995; Popović et al., 2001; Lodochnikova et al., 2013). They are, however, in the range of those measured in other

antimony(III) halide compounds (Ozturk et al., 2007, 2009, 2010). The C=S interatomic distance of the ligands suggests their coordination through their thionate forms.

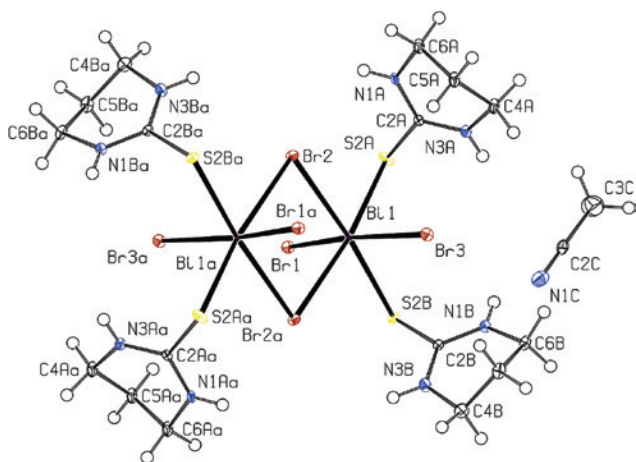


Figure 3: The molecular diagram of $\{[\text{BiBr}_2(\mu_2\text{-Br})(\text{tHPMT})_2]_2 \cdot \text{CH}_3\text{CN}\}$ (3).

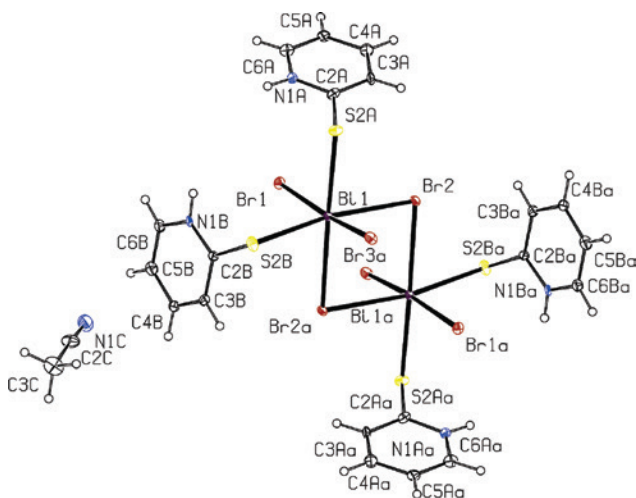


Figure 4: The molecular diagram of $\{[\text{BiBr}_2(\mu_2\text{-Br})(\text{PYT})_2]_2 \cdot \text{CH}_3\text{CN}\}$ (4).

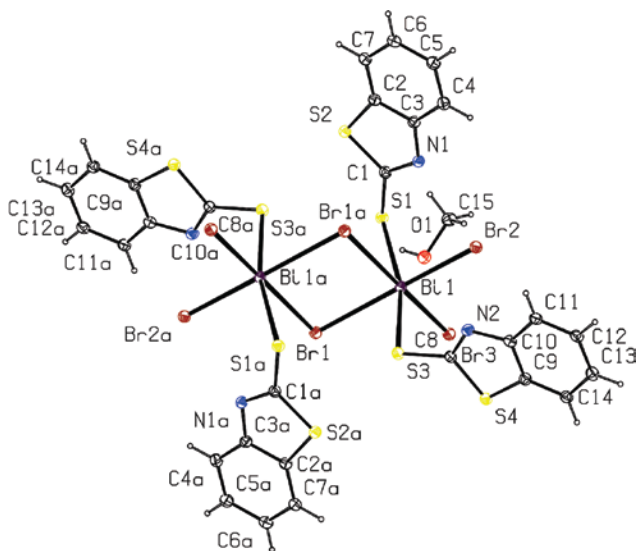


Figure 5: The molecular diagram of $\{[\text{BiBr}_2(\mu_2\text{-Br})(\text{MBZT})_2]_2 \cdot 2\text{CH}_3\text{OH}\}$ (5).

Biological studies

The *in vitro* antiproliferative activities of 1–5 were tested against the human adenocarcinoma breast (MCF-7) and cervix (HeLa) cells by SRB assay after their incubation for 48 hrs.

Compounds 1–5, exhibit moderate activity against the adenocarcinoma cells. The IC_{50} values of 4 against HeLa and MCF-7 cells are $6.5 \pm 0.7 \mu\text{M}$ and $9.7 \pm 1.0 \mu\text{M}$ respectively (Table 2). Therefore, the coordination of PYT enhances its biological activity. On the contrary, this is not observed when the rest of the ligands were used. Similarly, when bismuth(III) chloride complexes of the same thioamides (Yarar et al., 2018) were tested against the same cell lines, the corresponding one of the PYT exhibits the stronger activity once again. Among the bismuth(III) halide compounds of the thioamides tested (Table 2) against the HeLa and MCF-7 cells, a stronger activity is observed for the $\{[\text{BiCl}_3(\mu_2\text{-S-PYT})(\text{PYT})_2]\}$. A stronger activity of 4–5 has also been detected against HeLa than MCF-7 cells. The IC_{50} values of 5 are $15.0 \pm 1.1 \mu\text{M}$ and $>30 \mu\text{M}$, against the HeLa and MCF-7 cells, respectively. However, the cisplatin exhibits higher activity against the HeLa and MCF-7 cells than the study compounds 1–5. The IC_{50} values of the ligands are higher than $30 \mu\text{M}$ against the MCF-7 and HeLa cells.

The toxicities of 1–5 were studied against the non-cancerous cells MRC-5. The IC_{50} values of 1–3, 5 are higher than $30 \mu\text{M}$, indicating non-toxic behavior. However, the IC_{50} value of 4 against MRC-5 is $7.1 \pm 0.6 \mu\text{M}$, which is close to the corresponding one found against the HeLa and MCF-7 cells (6.5 ± 0.7 and $9.7 \pm 1.0 \mu\text{M}$, respectively) (Table 2). The therapeutic potency indexes ($\text{TPI} = \text{IC}_{50}(\text{normal cells}) / \text{IC}_{50}(\text{tumor cells})$) of 4 are 1.1 and 0.7 for the HeLa and MCF-7 cells respectively. In addition, 1–5 exhibit lower toxicity than cisplatin ($\text{IC}_{50} = 1.1 \pm 0.2 \mu\text{M}$). The IC_{50} values of the ligands against the MRC-5 cells are higher than $30 \mu\text{M}$.

In comparison, the bismuth(III)- dithiocarbamate complexes exhibit a significantly higher activity against both the HeLa and MCF-7 cells (Table 2). Their IC_{50} values lie between 0.023 and $0.33 \mu\text{M}$ (Yarar et al., 2018).

Study of the peroxidation of the linoleic acid by the enzyme lipoxygenase in the presence of bismuth(III) bromide complexes 1–5 and free thioamide ligands

LOXs are a group of oxidative enzymes with a non-heme iron atom in their active site (Haining and Axelrod, 1958; Knapp and Klinman, 2003); they are often associated with tumor cell proliferation, differentiation and

Table 2: The IC₅₀ values for cell viability found for the bismuth(III) complexes against the human adenocarcinoma cells HeLa (cervix), MCF-7 (breast) and MRC-5 cells (normal human fetal lung fibroblast cells).

Compounds	IC ₅₀ values (μM)				Reference
	LOX (μM)	HeLa	MCF-7	MRC-5	
{[BiBr ₂ (μ ₂ -Br)(MMI) ₂] ₂ · CH ₃ COCH ₃ · H ₂ O} (1)	66.7	>30	>30	>30	^a
{[BiBr ₂ (MBZIM) ₄] · Br · 2H ₂ O} (2)	48.8	>30	>30	>30	^a
{[BiBr ₂ (μ ₂ -Br)(tHPMT) ₂] ₂ · CH ₃ CN} (3)	65.3	>30	>30	>30	^a
{[BiBr ₂ (μ ₂ -Br)(PYT) ₂] ₂ · CH ₃ CN} (4)	176.8	6.5 ± 0.7	9.7 ± 1.0	7.1 ± 0.6	^a
{[BiBr ₂ (μ ₂ -Br)(MBZT) ₂] ₂ · 2CH ₃ OH} (5)	48.6	15.0 ± 1.1	>30	>30	^a
{[BiCl ₂ (μ ₂ -Cl)(MMI) ₂] ₂ · (CH ₃) ₂ CO}	68.2	>30	>30	11.2 ± 1.0	(Yarar et al., 2018)
{[BiCl ₂ (MBZIM) ₄] ⁺ · 2(Cl ⁻) · (H ₃ O ⁺) · 2H ₂ O}	57.0	>30	13.6	>30	(Yarar et al., 2018)
[BiCl ₃ (tHPMT) ₃]	67.2	>30	>30	>30	(Yarar et al., 2018)
{[BiCl ₃ (μ ₂ -S-PYT)(PYT) ₂]	169.5	6.1 ± 0.2	6.1 ± 0.2	4.7 ± 0.1	(Yarar et al., 2018)
[BiCl ₃ (MBZT) ₂] · H ₂ O}	57.0	>30	>30	>30	(Yarar et al., 2018)
MMI	377	>30	>30	>30	(Yarar et al., 2018)
MBZIM	286	>30	>30	>30	^a
tHPMT	286	>30	>30	>30	(Yarar et al., 2018)
PYT	1796	>30	>30	>30	(Yarar et al., 2018)
MBZT	188.3	>30	>30	>30	(Yarar et al., 2018)
{[BiBr(Me ₂ DTC) ₂] _n }		0.2 ± 0.01	0.08 ± 0.01	0.25 ± 0.01	(Arda et al., 2016)
{[BiBr ₂ (Et ₂ DTC)] _n }		0.2 ± 0.01	0.08 ± 0.006	0.32 ± 0.02	(Arda et al., 2016)
{[BiI ₂ (Me ₂ DTC)] _n }		0.3 ± 0.02	0.1 ± 0.003	0.29 ± 0.01	(Arda et al., 2016)
{[BiI(Et ₂ DTC) ₂] _n }		0.1 ± 0.01	0.05 ± 0.002	0.18 ± 0.01	(Arda et al., 2016)
{[BiI(μ ₂ -I)(Et ₂ DTC) ₂] _n }		0.05 ± 0.006	0.07 ± 0.008	0.15 ± 0.02	(Arda et al., 2016)
{[BiCl(Me ₂ DTC) ₂] _n }		0.33 ± 0.03	0.023 ± 0.003	–	(Ozturk et al., 2017)
{[Bi(Et ₂ DTC) ₃] _n }		0.19 ± 0.02	0.043 ± 0.008	–	(Ozturk et al., 2017)
cisplatin		3.9 ± 0.1	5.5 ± 0.4	1.1 ± 0.2	(Yarar et al., 2018)

^aThis work. Me₂DTC, Dimethyldithiocarbamate; Et₂DTC, diethyldithiocarbamate.

apoptosis (Samuelsson et al., 1987). Some evidence have proven the crucial role of LOX in cancer (Poyraz et al., 2011; Banti et al., 2016) as its inhibition induces apoptosis (Banti et al., 2016). The degree of LOX activity (A, %) in the presence of **1–5** was calculated according to the method described previously (Xanthopoulou et al., 2008; Ozturk et al., 2010; Poyraz et al., 2011). The effects of **1–5** and free thioamide ligands upon the oxidation of linoleic acid by the enzyme LOX were studied in a wide concentration range (Figure 6). The IC₅₀ values of **1–5** are 66.73 (**1**), 48.83 (**2**), 65.27 (**3**), 176.80 (**4**) and 48.58 μM (**5**), and for their free ligands, 377 (MMI), 286 (MBZIM), 219 (tHPMT), 1796 (PYT) and 188.3 μM (MBZT), respectively (Figure 7). The Bi(III) complexes **1–5** inhibit LOX activity in a moderate manner, which is in agreement with the antiproliferative studies as the compounds possess low cytotoxic activity. The IC₅₀ values of bromide bismuth(III) complexes against LOX are in accordance with the corresponding ones of their chloride analogues (Figure 7). Although **1–5** exhibit inhibitory activity against LOX; however, this is lower than the corresponding one of the organotin(IV) or silver(I) complexes (Xanthopoulou et al., 2008; Banti et al., 2016). This activity follows the relatively low cytotoxicity of these complexes.

Conclusions

In conclusion, five novel bismuth(III) bromide complexes with heterocyclic thioamide ligands have been successfully synthesized and characterized. The complexes of formulae {[BiBr₂(μ₂-Br)(MMI)₂]₂ · CH₃COCH₃ · H₂O} (**1**), {[BiBr₂(MBZIM)₄] · Br · 2H₂O} (**2**), {[BiBr₂(μ₂-Br)(tHPMT)₂]₂ · CH₃CN} (**3**), {[BiBr₂(μ₂-Br)(PYT)₂]₂ · CH₃CN} (**4**) and {[BiBr₂(μ₂-Br)(MBZT)₂]₂ · 2CH₃OH} (**5**) show versatile coordination modes. The molecular structures of complexes **1**, **3**, **4** and **5** are isostructural. These are the first examples of dinuclear bismuth(III) bromide compounds that have been structurally characterized with square pyramidal (SP) conformation around the metal center. The secondary Bi · · · (μ₂-Br) bonding interactions developed in **1**, **3**, **4** and **5** lead to octahedral arrangement (Oh). Moreover, the molecular structure of compound **2** is unique as it is the first ionic mononuclear octahedral bismuth(III) bromide complex.

Furthermore, the *in vitro* antiproliferative activity of **1–5** was tested against human adenocarcinoma breast (MCF-7) and cervix (HeLa) cells. Between the bromide compounds tested here, {[BiBr₂(μ₂-Br)(PYT)₂]₂ · CH₃CN} (**4**) exhibits the

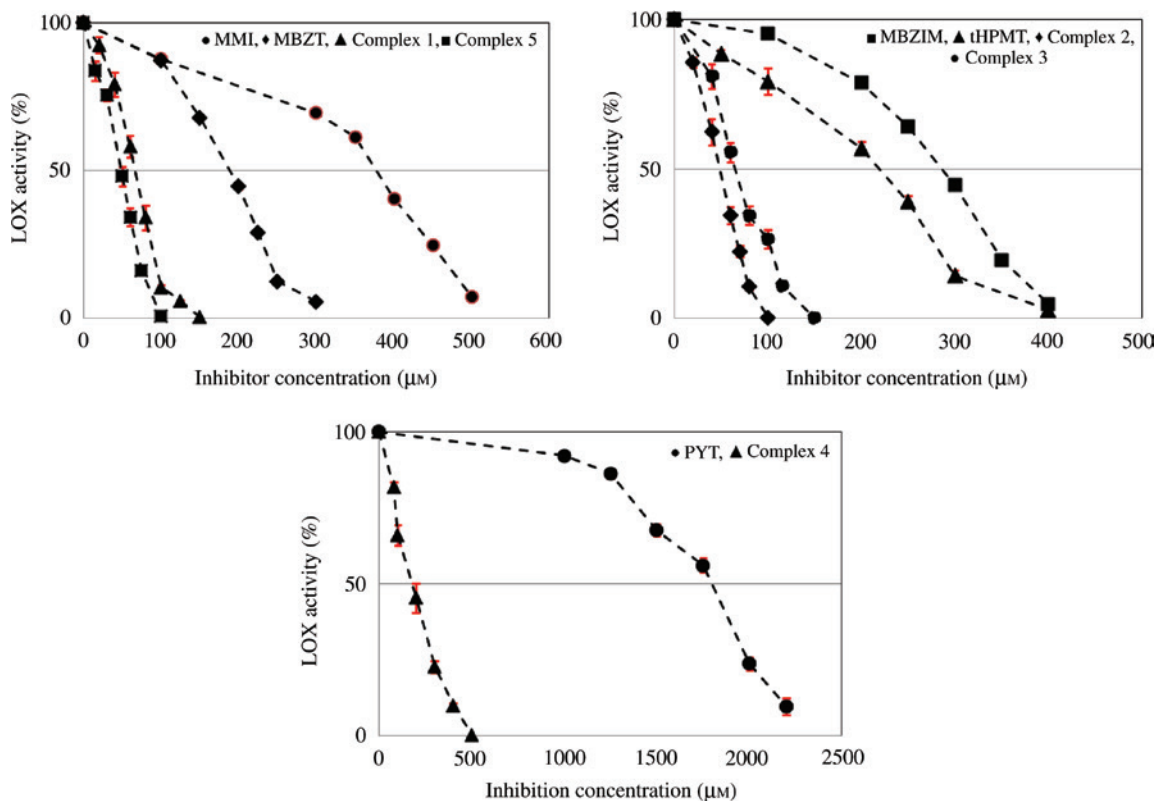


Figure 6: The inhibitory effects of 1–5 and thioamide ligands against LOX in various concentrations.

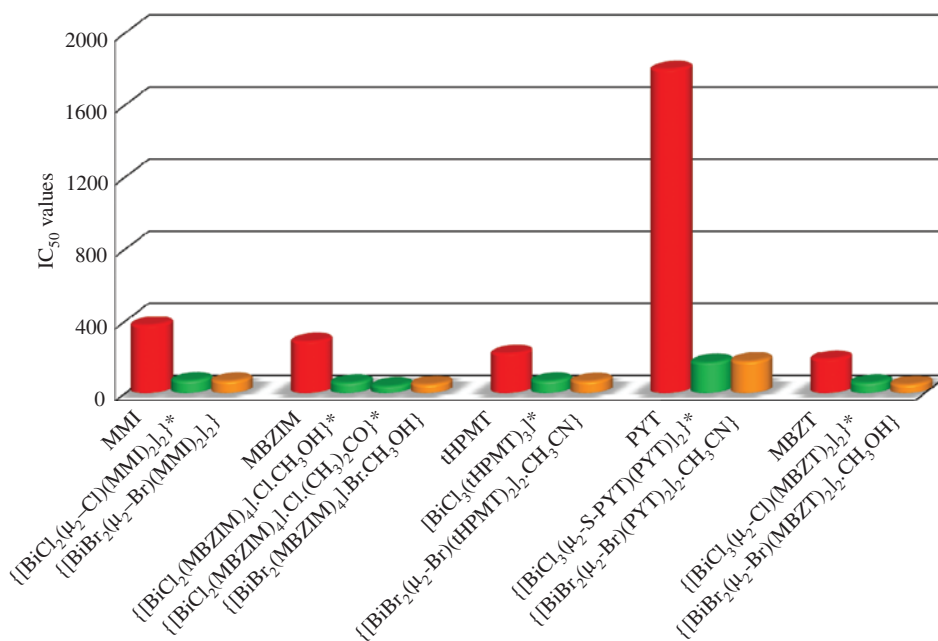


Figure 7: The IC_{50} values of the free thioamide ligands and bismuth(III) bromide and chloride against LOX.

lower IC_{50} values (stronger activity) against cells, which is comparable to the corresponding chloride ones (Table 2). Among the bismuth bromides and chloride complexes, those of 2-mercapto-pyridine 4 and $[(BiCl_3(\mu_2-S-PYT)(PYT)_2)]^*$

exhibit the strongest such activity (Table 2). Therefore, PYT enhances the biological activity, although the formation of octahedral arrangement around the metal centers is formed either by μ_2 -Br or μ_2 -S-PYT secondary binding interactions.

Furthermore, bismuth(III) compounds with dithiocarbamates exhibit significantly higher activity than those of heterocyclic thioamides, which in case of $\{[\text{BiCl}(\text{Me}_2\text{DTC})_2]_n\}$, increase even up to 250-fold than the corresponding one of cisplatin (Table 2). The inhibitory activity of the bromides or chloride bismuth(III) compounds against LOX follows their corresponding antiproliferative behaviour, thus confirming our assumption that this inhibition might be used as an indicator for the antiproliferative potential of a formulation (Xanthopoulou et al., 2008; Poyraz et al., 2011; Banti et al., 2016). In conclusion, based on the cell antiproliferative studies presented here, more efficient Bi(III) metallodrugs should be designed in the future within the class of dithiocarbamate ligands.

Experimental

Materials and instruments

All solvents used were of reagent grade. Bismuth(III) bromide (Merck, Darmstadt, Germany) and the 2-mercapto-1-methyl-imidazolidine (Sigma), 2-mercapto-benzimidazole (Merck, Darmstadt, Germany), 2-mercapto-3,4,5,6-tetrahydro-pyrimidine (Merck Darmstadt, Germany), 2-mercapto-pyridine (Merck, Darmstadt, Germany) and 2-mercapto-benzothiazole (Merck, Darmstadt, Germany) were used without further purification. The elemental analyses for C, H, N, and S were carried out with a Carlo Erba EA MODEL 1108 elemental analyzer (Milan, Italy). The melting points were measured in open tubes with a STUART SMP30 (Stone, Staffordshire, UK) scientific apparatus and were left uncorrected. The FT-IR spectra were recorded in the 4000–400 cm^{-1} region with Bruker Optics, Vertex 70 FT-IR spectrometer (Ettlingen, Germany) using ATR techniques. The far IR absorption spectra were recorded in 400–50 cm^{-1} using the FT-IR Bruker Equinox 55 spectrometer equipped with a Bruker Hyperion 1000 microscope (Ettlingen, Germany). Micro Raman spectra (64 scans) were recorded at room temperature using a low-power (~30 mW) green (514.5) nm laser on a Renishaw In Via spectrometer set at 2.0 resolution. The ^1H and ^{13}C NMR spectra were recorded with a Varian Unity Inova 500 MHz spectrometer (Palo Alto, CA, USA) in $\text{DMSO}-d_6$ with chemical shifts given in parts per million referenced to internal TMS (H). The molar conductivity of complexes in DMSO was measured by means of a VWR Phenomenal conductometer CO 3000 L (UK). The TG-DTA was carried out on a Seiko SII TG/DTA 7200 (Tokyo, Japan) apparatus under N_2 flow ($50 \text{ cm}^3 \text{ min}^{-1}$) with a heating rate of $10^\circ\text{C min}^{-1}$. The UV spectra were recorded in a Shimadzu UV-2600 UV-Vis spectrophotometer (Kyoto, Japan).

Synthesis and crystallization of the compounds

The $\{[\text{BiBr}_2(\mu_2\text{-Br})(\text{MMI})_2]_2 \cdot \text{CH}_3\text{COCH}_3 \cdot \text{H}_2\text{O}\}$ (**1**): 0.25 mmol bismuth(III) bromide (0.112 g) and 0.50 mmol 2-mercapto-1-methyl-imidazole (0.057 g) were dissolved in 10 mL acetone, respectively. The resulting solution was stirred at room temperature for 4 h. The

obtained solution was filtered. The clear orange solution was kept in darkness at room temperature. One week later, orange crystals suitable for single crystal XRD data were obtained.

1: Orange crystals; yield 85%; melting point: 118–120°C; $M_w = 1430.10 \text{ g/mol}$. Elemental analysis: found C=14.22; H=1.73; N=8.17; S=9.41%, calculated (without solvent molecules) for $\text{C}_{16}\text{H}_{24}\text{Bi}_2\text{Br}_6\text{N}_8\text{S}_4$: C=14.19; H=1.78; N=8.28; S=9.47%. Mid-IR (cm^{-1}): 3130 w, 1701 w, 1689 w, 1570 s, 1508 w, 1468 m, 1443 m, 1408 w, 1354 m, 1284 m, 1229 w, 1157 s, 1088 m, 1020 w, 920 m, 878 w, 779 w, 743 s, 669 s, 609 w, 527 w, 511 m, 473 w, 405 w. Soluble in acetonitrile, acetone, tetrahydrofuran, dimethylsulfoxide. UV-Vis (DMSO): λ_{max} ($\log\epsilon$) = 266 (4.87) and 304 (4.05). Λ_{M} (DMSO): $23.6 \Omega^{-1}\text{cm}^2\text{mol}^{-1}$.

$\{[\text{BiBr}_2(\text{MBZIM})_4] \cdot \text{Br} \cdot 2\text{H}_2\text{O}\}$ (**2**): A solution of bismuth(III) bromide (0.112 g, 0.25 mmol) in acetonitrile (10 cm^3) was added to the solution of 2-mercaptobenzimidazole (0.077 g, 0.50 mmol) in methanol (10 cm^3). The resulting yellow solution was stirred at room temperature for 3 h. The obtained solution was filtered. The clear yellow solution was kept in darkness at room temperature. Two weeks later, red crystals suitable for single crystal XRD data were obtained.

2: Red crystals; yield 89%; melting point: 228–231°C; $M_w = 1085.48 \text{ g/mol}$. Elemental analysis: found C=32.09; H=2.27; N=10.57; S=12.09%; calculated (without solvent molecules) for $\text{C}_{28}\text{H}_{24}\text{BiBr}_3\text{N}_8\text{S}_4$: C=32.05; H=2.30; N=10.68; S=12.22%. Mid-IR (cm^{-1}): 3544 w, 3068 w, 1616 w, 1591 m, 1541 w, 1491 s, 1148 s, 1389 w, 1346 s, 1254 w, 1219 w, 1169 m, 1148 w, 1111 w, 1005 m, 972 m, 856 w, 814 w, 752 s, 741 s, 619 w, 598 s, 467 m, 413 m. UV-Vis (DMSO): λ_{max} ($\log\epsilon$) = 250.5 (4.68), 312.5 (5.14). Soluble in methanol, ethanol, acetonitrile, acetone, tetrahydrofuran, dimethylsulfoxide. Λ_{M} (DMSO): $13.9 \Omega^{-1}\text{cm}^2\text{mol}^{-1}$.

$\{[\text{BiBr}_2(\mu_2\text{-Br})(\text{tHPMT})_2]_2 \cdot \text{CH}_3\text{CN}\}$ (**3**): A solution of 2-mercapto-3,4,5,6-tetrahydro-pyrimidine (0.058 g, 0.50 mmol) in methanol (10 cm^3) was added to a solution of bismuth(III) bromide (0.112 g, 0.25 mmol) in acetonitrile (10 cm^3). The resulting yellow solution was stirred at room temperature for 30 min. The obtained solution was filtered. The clear yellow solution was kept in darkness at room temperature. One-week later, yellow crystals suitable for single crystal XRD data were obtained.

3: Yellow crystals; yield 86%; melting point: 113–116°C; $M_w = 1403.18 \text{ g/mol}$. Elemental analysis: found C=15.38; H=2.47; N=9.05; S=9.09% calculated for $\text{C}_{18}\text{H}_{35}\text{Bi}_2\text{Br}_6\text{N}_9\text{S}_4$: C=15.41; H=2.51; N=8.98; S=9.14%. Mid-IR (cm^{-1}): 3342 w, 3265 m, 1595 s, 1539 s, 1421 w, 1410 m, 1360 m, 1315 m, 1203 s, 1111 w, 1067 w, 972 w, 937 w, 876 w, 808 m, 687 m, 623 m, 563 m, 540 m, 517 m, 410 m. UV-Vis (DMSO): λ_{max} ($\log\epsilon$) = 257 (4.83) and 298 (4.09). Soluble in acetonitrile, acetone, tetrahydrofuran, dimethylsulfoxide. Λ_{M} (DMSO): $18.8 \Omega^{-1}\text{cm}^2\text{mol}^{-1}$.

$\{[\text{BiBr}_2(\mu_2\text{-Br})(\text{PYT})_2]_2 \cdot \text{CH}_3\text{CN}\}$ (**4**): A solution of 2-mercapto-pyridine (0.055 g, 0.50 mmol) in methanol (10 cm^3) was added to a solution of bismuth(III) bromide (0.112 g, 0.25 mmol) in acetonitrile (10 cm^3). The resulting yellow solution was stirred at room temperature for 30 min. The obtained solution was filtered. The clear orange solution was kept in darkness at room temperature. Two weeks later, yellow crystals suitable for single crystal XRD data were obtained.

4: Yellow crystals; yield 89%; melting point: 118–120°C; $M_w = 1383.10 \text{ g/mol}$. Elemental analysis: found C=19.18; H=1.71; N=5.13; S=9.32%; calculated for $\text{C}_{22}\text{H}_{23}\text{Bi}_2\text{Br}_6\text{N}_5\text{S}_4$: C=19.10; H=1.68; N=5.06; S=9.27%. Mid-IR (cm^{-1}): 3169 w, 1655 w, 1603 m, 1574 s, 1508 m, 1443 m, 1396 w, 1365 m, 1340 w, 1256 m, 1161 m, 1124 s, 1105 m, 1082 m, 1034 m, 1001 w, 897 w, 862 w, 752 s, 721 s, 619 m, 559 w, 484 m, 434 m. UV-Vis (DMSO): λ_{max} ($\log\epsilon$) = 256 (4.70), 293 (4.72)

and 363 (4.28). Soluble in acetonitrile, acetone, dimethylsulfoxide. Λ_M (DMSO): $8.7 \Omega^{-1} \text{ cm}^2 \text{ mol}^{-1}$.

$\{[\text{BiBr}_2(\mu_2\text{-Br})(\text{MBZT})_2]_2 \cdot 2\text{CH}_3\text{OH}\}$ (5): A solution of 2-mercapto-benzothiazole (0.060 g, 1.00 mmol) was added to a solution of bismuth(III) bromide (0.224 g, 0.50 mmol) in methanol (10 cm^3). The resulting red solution was stirred at 50°C for 4 h. The obtained solution was filtered. The clear red solution was kept in darkness at room temperature. Twelve days later, red crystals suitable for single crystal XRD data were obtained.

5: Red crystals; yield 83%; melting point: 189–192°C; Mw=1630.41 g/mol. Elemental analysis: found: C=21.82; H=1.57; N=3.48; S=16.10%; calculated for $\text{C}_{30}\text{H}_{28}\text{Bi}_2\text{Br}_6\text{N}_4\text{O}_2\text{S}_8$: C=21.79; H=1.51; N=3.51; S=16.05%. Mid-IR (cm^{-1}): 3.188 w, 1601 w, 1522 w, 1491 m, 1423 m, 1356 w, 1331 m, 1281 w, 1250 w, 1153 w, 1130 w, 1078 m, 1022 s, 1007 s, 939 m, 866 m, 176 s, 679 m, 600 m, 561 m, 501 w, 422 m. UV-Vis (DMSO): λ_{max} ($\log \epsilon$) = 257 (4.65) and 327.5 (5.07). Soluble in methanol, ethanol, acetonitrile, acetone, tetrahydrofuran, dimethylsulfoxide. Λ_M (DMSO): $23.4 \Omega^{-1} \text{ cm}^2 \text{ mol}^{-1}$.

X-ray structure determination

Single crystal XRD diffraction data for **1**, **2** and **5** were collected on an Oxford-Diffraction Supernova diffractometer, equipped with a CCD area detector utilizing Cu K α ($\lambda = 1.5418 \text{ \AA}$) radiation. A suitable crystal was mounted on a Hampton cryoloop with Paratone-N oil and transferred to a goniostat where it was cooled for data collection. The empirical absorption corrections (multiscan based on symmetry-related measurements) were applied using the CrysAlis RED software (Oxford-Diffraction). The structures were solved by direct methods using the SIR2004 (Burla et al., 2005) and refined on F^2 using the full-matrix least-squares with SHELXL-2014/7 (Sheldrick, 2014). The software packages used were as follows: CrysAlis CCD for data collection (Oxford Diffraction) CrysAlis RED for cell refinement and data reduction (Oxford Diffraction) WINGX for geometric calculations (Farrugia, 1999) and ORTEP for molecular

graphics. The non-H atoms were treated anisotropically, whereas the aromatic H atoms were placed in calculated, ideal positions and refined as riding on their respective carbon atoms. Crystal data for **3** and **4** were measured on a KUMA KM4CCD four-circle diffractometer (CrysAlis CCD) equipped with a CCD detector using the graphite-monochromated MoKa radiation ($\lambda = 0.71073 \text{ \AA}$). Cell parameters were determined by the least-squares refinement of the diffraction data from 25 reflections (CRYALIS RED). All data were corrected for the Lorentz-polarization effects and absorption (CRYALIS RED; Sheldrick, 1990). The structures were solved with direct methods with SHELXS97 (Sheldrick, 1990) and refined by full-matrix least-squares procedures on F^2 with SHELXL97 (Sheldrick, 1997). All non-hydrogen atoms were refined anisotropically. The hydrogen atoms were located at the calculated positions and then refined via the ‘riding model’ with isotropic thermal parameters fixed at 1.2 (1.3 for CH_3 groups). The experimental crystallographic data for **1–5** are provided in Table 3. The structure determination of **2** and **5** ended up in quite large R-factors. This is due to twin crystals. However, despite the high R-factors, the refinement of the data resulted in the safe formulae for these compounds. These are then used for the solution preparation for the biological experiments, which is the main aim of this work.

Supplementary data are available from CCDC, 12 Union Road, Cambridge CB2 1EZ, UK, (e-mail: mailto:deposit@ccdc.cam.ac.uk), on request, quoting the deposition numbers CCDC 1831830 (**1**), 1831829 (**2**), 1832427 (**3**), 1832428 (**4**) and 1831828 (**5**).

Biological tests

Biological experiments were carried in dimethyl sulfoxide Dulbecco’s Modified Eagle’s Medium solutions (DMEM) DMSO/DMEM (0.02%–0.2% v/v) for the complexes **1–5**. The stock solutions of the complexes **1–5**, (0.01 M) in DMSO were freshly prepared and diluted in a cell culture medium to the desired concentrations (0.5–30 μM). The results are expressed in terms of IC_{50} values, that is, the concentration

Table 3: The experimental crystallographic data for the bismuth(III) bromide complexes **1–5**.

	1	2	3	4	5
Empirical formula	$\text{C}_{19}\text{H}_{32}\text{Bi}_2\text{Br}_6\text{N}_8\text{O}_2\text{S}_4$	$\text{C}_{28}\text{H}_{28}\text{BiBr}_3\text{N}_8\text{O}_2\text{S}_4$	$\text{C}_{18}\text{H}_{35}\text{Bi}_2\text{Br}_6\text{N}_9\text{S}_4$	$\text{C}_{22}\text{H}_{23}\text{Bi}_2\text{Br}_6\text{N}_5\text{S}_4$	$\text{C}_{30}\text{H}_{28}\text{Bi}_2\text{Br}_6\text{N}_4\text{O}_2\text{S}_8$
Formula weight (g/mol)	1430.10	1085.48	1403.18	1383.10	1630.41
T (K)	100(2)	100(2)	100(2)	130(2)	100(2)
Crystal System	Orthorhombic	Monoclinic	Monoclinic	Monoclinic	Triclinic
Space group	$Cmc2_1$	$P2_1/c$	$C2/c$	$C2/c$	$P\bar{1}$
a (\AA)	13.8330(4)	13.8222(4)	23.375(2)	23.225(3)	10.1610(8)
b (\AA)	13.6238(4)	17.0677(5)	12.9498(6)	13.2014(6)	10.2461(8)
c (\AA)	20.5347(7)	7.7883(2)	15.8095(14)	16.1799(5)	10.6154(10)
α (deg)	90	90	90	90	90.325(7)
β (deg)	90	98.518(3)	127.987(14)	131.53(3)	91.768(7)
γ (deg)	90	90	90	90	94.071(7)
V (\AA^3)	3869.9(2)	1817.10(9)	3771.7(9)	3713.7(18)	1101.83(16)
Z	4	2	4	4	1
ρ calcd (g/cm^3)	2.444	1.962	2.543	2.547	2.451
μ (mm^{-1})	27.184	15.860	15.927	28.274	25.700
R, wR, S	0.0263, 0.0713, 1.057	0.1027, 0.2647, 1.168	0.0438, 0.1147, 0.98	0.0439, 0.0948, 1.02	0.0910, 0.2256, 1.153

of drug required to inhibit cell growth by 50% compared to control, after of 48 h incubation of the complexes towards cell lines. The cell viability was determined by SRB assay, as previously described (Banti et al., 2016).

Lipoxygenase activity inhibition

This was performed as previously reported (Xanthopoulou et al., 2008).

Acknowledgements: (a) I.I.O. and M.Ç. acknowledge the financial support from The Scientific and Technological Research Council of Turkey (TUBITAK, Project No. 114Z457). (b) CNB and SKH would like to thank the Unit of Bioactivity Testing of Xenobiotics of the University of Ioannina for providing access to their facilities. (c) The International Graduate Program in ‘Biological Inorganic Chemistry’, which operates at the University of Ioannina within the collaboration of the Departments of Chemistry of the Universities of Ioannina, Athens, Thessaloniki, Patras, Crete and the Department of Chemistry of the University of Cyprus (<http://bic.chem.uoi.gr/BIC-En/index-en.html>), is acknowledged for the stimulating discussion forum.

References

- Arda, M.; Ozturk, I. I.; Banti, C. N.; Kourkoumelis, N.; Manoli, M.; Tasiopoulos, A. J.; Hadjikakou, S. K. Novel bismuth compounds: synthesis, characterization and biological activity against human adenocarcinoma cells. *RSC Adv.* **2016**, *6*, 29026–29044.
- Balas, V. I.; Verginadis, I. I.; Geromichalos, G. D.; Kourkoumelis, N.; Male, L.; Hursthouse, M. B.; Repana, K. H.; Yiannaki, E.; Charalabopoulos, K.; Bakas, T.; et al. Synthesis, structural characterization and biological studies of the triphenyltin(IV) complex with 2-thiobarbituric acid. *Eur. J. Med. Chem.* **2011**, *46*, 2835–2844.
- Banti, C. N.; Papatriantafyllopoulou, C.; Manoli, M.; Tasiopoulos, A. J.; Hadjikakou, S. K. Nimesulide silver metallodrugs, containing the mitochondriotropic, triaryl derivatives of pnictogen; Anticancer activity against human breast cancer cells. *Inorg. Chem.* **2016**, *55*, 8681–8696.
- Burla, M. C.; Caliendo, R.; Camalli, M.; Carrozzini, B.; Cascarano, G. L.; De Caro, L.; Giacovazzo, C.; Polidori, G.; Spagna, R. SIR2004: an improved tool for crystal structure determination and refinement. *J. Appl. Cryst.* **2005**, *38*, 381–388.
- CrysAlis CCD, version 1.171.31.5; Oxford Diffraction Ltd. (release 28-08-2006 CrysAlis171.NET).
- CRYALIS RED, Version 1.171.31.5 (release 28–08–2006 CrysAlis 171.NET); Oxford Diffraction, Ltd.
- Farrugia, L. J. WinGX and ORTEP for Windows: an update. *J. Appl. Cryst.* **1999**, *32*, 837–838.
- Hadjikakou, S. K.; Antoniadis, C. D.; Hadjiliadis, N.; Kubicki, M.; Binolis, J.; Karkabounas, S.; Charalabopoulos, K. Synthesis and characterization of new water stable antimony(III) complex with pyrimidine-2-thione and *in vitro* biological study. *Inorg. Chim. Acta* **2005**, *358*, 2861–2866.
- Haining, J. L.; Axelrod, B. Induction period in the lipoxidase-catalyzed oxidation of linoleic acid and its abolition by substrate peroxide. *J. Biol. Chem.* **1958**, *232*, 193–202.
- Knapp, M. J.; Klinman, J. P. Kinetic studies of oxygen reactivity in soybean lipoxygenase-1. *Biochemistry* **2003**, *42*, 11466–11475.
- Li, M.; Li, R. K. Two new bismuth thiourea bromides: crystal structure, growth, and characterization. *Dalton Trans.* **2014**, *43*, 2577–2580.
- Li, M.; Lu, Y.; Yang, M.; Li, Y.; Zhang, L.; Xie, S. One dodecahedral bismuth(III) complex derived from 2-acetylpyridine N(4)-pyridylthiosemicarbazone: synthesis, crystal structure and biological evaluation. *Dalton Trans.* **2012a**, *41*, 12882.
- Li, M.-X.; Yang, M.; Niu, J.-Y.; Zhang, L.-Z.; Xie, S.-Q. A nine-coordinated bismuth(III) complex derived from pentadentate 2,6-diacetylpyridine bis((4)N-methylthiosemicarbazone): crystal structure and both *in vitro* and *in vivo* biological evaluation. *Inorg. Chem.* **2012b**, *51*, 12521–12526.
- Lodochnikova, O. A.; Bodrov, A. V.; Saifina, A. F.; Nikitina, L. E.; Litvinov, I. A. A new polymorph of methimazole: Single crystal and powder X-ray diffraction study. *J. Struct. Chem.* **2013**, *54*, 140–147.
- Ohms, U.; Guth, H.; Kutoglu, A.; Scherlinger, C. 2-Thiopyridone: X-ray and neutron diffraction study. *Acta Cryst.* **1982**, *B38*, 831–834. Oxford Diffraction. CrysAlis CCD and CrysAlis RED; Oxford Diffraction Ltd.: Abingdon, UK, 2008.
- Ozturk, I. I.; Hadjikakou, S. K.; Hadjiliadis, N.; Kourkoumelis, N.; Kubicki, M.; Baril, M.; Butler, I. S.; Balzarini, J. Synthesis, structural characterization, and biological studies of new antimony(III) complexes with thiones. The influence of the solvent on the geometry of the complexes. *Inorg. Chem.* **2007**, *46*, 8652–8661.
- Ozturk, I. I.; Hadjikakou, S. K.; Hadjiliadis, N.; Kourkoumelis, N.; Kubicki, M.; Tasiopoulos, A. J.; Scleiman, H.; Barsan, M. M.; Butler, I. S. New antimony(III) bromide complexes with thioamides: synthesis, characterization, and cytostatic properties. *Inorg. Chem.* **2009**, *48*, 2233–2245.
- Ozturk, I. I.; Filimonova, S.; Hadjikakou, S. K.; Kourkoumelis, N.; Dokorou, V.; Manos, M. J.; Tasiopoulos, A. J.; Barsan, M. M.; Butler, I. S.; Milaeva, E. R.; et al. Structural motifs and biological studies of new antimony(III) iodide complexes with thiones. *Inorg. Chem.* **2010**, *49*, 488–501.
- Ozturk, I. I.; Kourkoumelis, N.; Hadjikakou, S. K.; Manos, M. J.; Tasiopoulos, A. J.; Butler, I. S.; Balzarini, J.; Hadjiliadis, N. Interaction of antimony(III) chloride with thiourea, 2-mercapto-5-methyl-benzimidazole, 3-methyl-2-mercaptobenzothiazole, 2-mercaptopyrimidine, and 2-mercaptopyridine. *J. Coord. Chem.* **2011**, *64*, 3859–3871.
- Ozturk, I. I.; Banti, C. N.; Manos, M. J.; Tasiopoulos, A. J.; Kourkoumelis, N.; Charalabopoulos, K.; Hadjikakou, S. K. Synthesis, characterization and biological studies of new antimony(III) halide complexes with ω -thiocaprolactam. *J. Inorg. Biochem.* **2012a**, *109*, 57–65.
- Ozturk, I. I.; Metsios, A. K.; Filimonova-Orlova, S.; Kourkoumelis, N.; Hadjikakou, S. K.; Manos, E.; Tasiopoulos, A. J.; Karkabounas, S.; Milaeva, E. R.; Hadjiliadis, N. Study on single crystal struc-

- ture of the antimony(III) bromide complex with 3-methyl-2-mercaptobenzothiazole and biological activity of some antimony(III) bromide complexes with thioamides. *Med. Chem. Res.* **2012b**, *21*, 3523–3531.
- Ozturk, I. I.; Urgut, O. S.; Banti, C. N.; Kourkoumelis, N.; Owczarzak, A. M.; Kubicki, M.; Charalabopoulos, K.; Hadjikakou, S. K. Synthesis, structural characterization and cytotoxicity of the antimony(III) chloride complex with N,N-Dicyclohexyldithiooxamide. *Polyhedron* **2013**, *52*, 1403–1410.
- Ozturk, I. I.; Banti, C. N.; Kourkoumelis, N.; Manos, M. J.; Tasiopoulos, A. J.; Owczarzak, A. M.; Kubicki, M.; Hadjikakou, S. K. Synthesis, characterization and biological activity of antimony(III) or bismuth(III) chloride complexes with dithiocarbamate ligands derived from thiuram degradation. *Polyhedron* **2014a**, *67*, 89–103.
- Ozturk, I. I.; Urgut, O. S.; Banti, C. N.; Kourkoumelis, N.; Owczarzak, A. M.; Kubicki, M.; Hadjikakou, S. K. Synthesis, structural characterization and cytostatic properties of N,N-dicyclohexyldithiooxamide complexes of antimony(III) halides (SbX₃, X: Br or I). *Polyhedron* **2014b**, *70*, 172–179.
- Ozturk, I. I.; Yazar, S.; Banti, C. N.; Kourkoumelis, N.; Chrysouli, M. P.; Manoli, M.; Tasiopoulos, A. J.; Hadjikakou, S. K. QSAR studies on antimony(III) halide complexes with N-substituted thiourea derivatives. *Polyhedron* **2017**, *123*, 152–161.
- Popović, Z.; Matković-Čalogović, D.; Pavlović, G.; Soldin Ž.; Giester, G.; Rajić, M.; Vikić-Topić, D. Preparation, thermal analysis and spectral characterization of the 1:1 complexes of mercury(II) halides and pseudohalides with 3,4,5,6-tetrahydropyrimidine-2-thione. Crystal structures of Bis(3,4,5,6-tetrahydropyrimidine-2-thione-S)mercury(II) tetrachloro and tetrabromomercurate(II). *Croat. Chem. Acta* **2001**, *74*, 359–380.
- Poyraz, M.; Banti, C. N.; Kourkoumelis, N.; Dokorou, V.; Manos, M. J.; Simčić, M.; Golič-Grdadolnik, S.; Mavromoustakos, T.; Giannoulis, A. D.; Verginadis, I. I.; et al. Synthesis, structural characterization and biological studies of novel mixed ligand Ag(I) complexes with triphenylphosphine and aspirin or salicylic acid. *Inorg. Chim. Acta* **2011**, *375*, 114–121.
- Ravikuma, K.; Mohan, K. C.; Bidasagar, M.; Swamy, G. Y. S. K. Crystal structure of 2-mercaptobenzimidazole and bis[2-mercaptobenzimidazole]dichlorocobalt(II). *J. Chem. Crystallogr.* **1995**, *25*, 325–329.
- Samuelsson, B.; Dahlen, S. E.; Lindgren, J.; Rouzer, C. A.; Serhan, C. N. Leukotrienes and lipoxins: structures, biosynthesis, and biological effects. *Science* **1987**, *237*, 1171–1176.
- Sheldrick, G. M. Phase annealing in SHELX-90: direct methods for larger structures. *Acta Crystallogr.* **1990**, *A 46*, 467–473.
- Sheldrick, G. M. SHELXL-97, Program for the Refinement of Crystal Structures; University of Göttingen: Göttingen, Germany, 1997.
- Sheldrick, G. M. SHELXL-2014/7, Program for Refinement of Crystal Structures; University of Göttingen: Germany, 2014.
- Shpakovsky, D. B.; Banti, C. N.; Beaulieu-Houle, G.; Kourkoumelis, N.; Manoli, M.; Manos, M. J.; Tasiopoulos, A. J.; Hadjikakou, S. K.; Milaeva, E. R.; Charalabopoulos, K.; et al. Synthesis, structural characterization and *in vitro* inhibitory studies against human breast cancer of the bis-(2,6-di-*tert*-butylphenol)tin(IV) dichloride and its complexes. *Dalton Trans.* **2012**, *41*, 14568–14582.
- Srinivas, K.; Suresh, P.; Babu, C. N.; Sathyanarayana, A.; Prabusankar, G. Heavier chalcogenone complexes of bismuth(III) trihalides: potential catalysts for acylative cleavage of cyclic ethers. *RSC Adv.* **2015**, *5*, 15579–15590.
- Srinivas, K.; Sathyanarayana, A.; Babu, C. N.; Prabusankar, G. Bismuth(III)dichalcogenones as highly active catalysts in multiple C–C bond formation reactions. *Dalton Trans.* **2016**, *45*, 5196–5209.
- Urgut, O. S.; Ozturk, I. I.; Banti, C. N.; Kourkoumelis, N.; Manoli, M.; Tasiopoulos, A. J.; Hadjikakou, S. K. New antimony(III) halide complexes with dithiocarbamate ligands derived from thiuram degradation: the effect of the molecule's close contacts on *in vitro* cytotoxic activity. *Mater. Sci. Eng. C* **2016a**, *58*, 396–408.
- Urgut, O. S.; Ozturk, I. I.; Banti, C. N.; Kourkoumelis, N.; Manoli, M.; Tasiopoulos, A. J.; Hadjikakou, S. K. Addition of tetraethylthiuram disulfide to antimony(III) iodide; synthesis, characterization and biological activity. *Inorg. Chim. Acta* **2016b**, *443*, 141–150.
- Xanthopoulou, M. N.; Hadjikakou, S. K.; Hadjiliadis, N.; Milaeva, E. R.; Gracheva, J. A.; Tyurin, V. Yu.; Kourkoumelis, N.; Christoforidis, K. C.; Metsios, A. K.; Karkabounas, S.; et al. Biological studies of new organotin(IV) complexes of thioamide ligands. *Eur. J. Med. Chem.* **2008**, *43*, 327–335.
- Yang, N.; Sun, H. Biocoordination chemistry of bismuth: recent advances. *Coord. Chem. Rev.* **2007**, *251*, 2354–2366.
- Yazar, S.; Ozturk, I. I.; Banti, C. N.; Panagiotou, N.; Papatriantafyllou, C.; Manoli, M.; Manos, M. J.; Tasiopoulos, A. J.; Hadjikakou, S. K. Synthesis, characterization and cytostatic properties of bismuth(III) chloride complexes with heterocyclic thioamides; A survey for structure activity relationship. *Inorg Chim Acta* **2018**, *471*, 23–33.
- Zhang, N.; Tai, Y.; Li, M.; Ma, P.; Zhao, J.; Niu, J. Main group bismuth(III), gallium(III) and diorganotin(IV) complexes derived from bis(2-acetylpyrazine)thiocarbonohydrazone: synthesis, crystal structures and biological evaluation. *Dalton Trans.* **2014**, *43*, 5182–5189.

Supplementary Material: The online version of this article offers supplementary material (<https://doi.org/10.1515/mgmc-2018-0035>).